



# POLITECNICO

## MILANO 1863

Department of Aerospace Science and Technology

Master of Science in Space Engineering

Orbital Mechanics

A.Y. 2023/2024

Dr. C. Colombo

## Assignments Report

**Group ID: 2301**

Ignesti Samuele - 252334 - 10736840  
Guglielmo Gualdana - 247250 - 10695552  
Martina Angela Vurro - 243142 - 11009775  
Adam Lakrad - 244907 - 10727361

January 2024

## Contents

<b>1</b>	<b>Introduction</b>	<b>2</b>
<b>2</b>	<b>Interplanetary mission design</b>	<b>2</b>
2.1	Requirements . . . . .	2
2.2	Design Process and Implemented Methods . . . . .	2
2.2.1	The design problem . . . . .	2
2.2.2	Domain . . . . .	3
2.2.3	A brute force approach . . . . .	4
2.2.4	Particles Swarm optimisations . . . . .	4
2.2.5	Genetic Algorithms . . . . .	5
2.3	Results and best option . . . . .	5
2.3.1	Tangential manoeuvre . . . . .	5
2.3.2	Deep Space and Non Tangential manoeuvres . . . . .	6
<b>3</b>	<b>Planetary observation mission</b>	<b>7</b>
3.1	Requirements . . . . .	7
3.2	Initial orbit characterisation . . . . .	7
3.3	Ground track repeating orbit characterisation . . . . .	8
3.4	Orbital elements propagation and filtering . . . . .	9
3.4.1	Cartesian coordinates VS Gauss planetary equations . . . . .	10
3.4.2	Filtering . . . . .	10
3.5	Comparison with real data . . . . .	11

## Nomenclature and Constants

SYMBOL	MEANING
$\mathbb{J}$	Jupiter
$\mathbb{M}$	Mercury
$\oplus$	Earth
$\mathbb{M}$	Moon
$\odot$	Sun
$a$	Semi-major axis
$e$	Eccentricity
$i$	Inclination
$\Omega$	RAAN Right Ascension of Ascending Node
$\omega$	Pericentre anomaly
$\theta$	True anomaly
$\delta$	Turning angle
$r_p$	Pericentre radius
$\lambda$	Longitude
$M$	Mean anomaly
$n$	Mean angular velocity
$P_\Omega$	Nodal period
FFT	Fast Fourier Transform
GA	Genetic Algorithm
PGA	Powered Gravity Assist
PSO	Particle Swarm Optimisation
SOI	Sphere of Influence
SRP	Solar Radiation Pressure
TNH	Tangential-normal-out of plane
TOF	Time of flight
$t_d$	Time of departure
$t_a$	Time of arrival
$t_{PGA}$	Time of Powered Gravity Assist
$\mathbf{V}$	Velocity with respect to Sun
$\mathbf{v}$	Velocity with respect to planet

SYMBOL	MEANING
AU	Astronomical Unit
R	Planet radius
$\mu$	Planetary constant
$C_r$	Reflectivity coefficient
$J_2$	Second zonal harmonic

# 1 Introduction

The PoliMi Space Agency is currently working on two missions: an *Interplanetary Explorer Mission* visiting three planets in the Solar System and a *Planetary Explorer Mission* performing Earth observation. As part of the mission analysis team we are requested to perform the preliminary studies and carry out a report of the results for both missions.

# 2 Interplanetary mission design

"The PoliMi Space Agency is carrying out a feasibility study for a potential Interplanetary Explorer Mission visiting three planets in the Solar System. As part of the mission analysis team, you are requested to perform the preliminary mission analysis. You have to study the transfer options from the departure planet to the arrival planet, with a powered gravity assist (flyby) at the intermediate planet, and propose a solution based on the mission cost (measured through the total  $\Delta V$ ). The departure, flyby, and arrival planets have been decided by the science team. Constraints on earliest departure and latest arrival have also been set by the launch provider. The systems engineering team, and the Agency's leadership."

## 2.1 Requirements

In the feasibility study of the Interplanetary mission design, it has been selected from the agency the period of time in which the mission need to be accomplished, the starting and the arrival planet, and it has been asked also to take in consideration the chance to use the influence of another planet through a power gravity assist manoeuvre on the proximity of the planet, in order to optimise the transfer in terms of total  $\Delta V$ . By describing the problem trough the patched conic method, it is possible to approach the problem with a much lower complexity level, keeping a good approximation of the reality. In Table 1, requirements are listed:

Earliest Departure	01.01.2028 00:00:00
Latest Arrival	01.01.2058 00:00:00
Starting planet	Mercury
Arrival planet	Jupiter
Gravity assist planet	Earth

Table 1: Requirements

## 2.2 Design Process and Implemented Methods

### 2.2.1 The design problem

The required objective translates mathematically into an optimisation problem of a function. in our case the function to be optimised indicates the total cost of the transfer. Thanks to the patched conics approach the problem depends on three variables only: the time of departure from Mercury  $t_d$ , the arrival time on the Earth proximity  $t_{PGA}$  and the arrival time in the proximity of Jupiter  $t_a$ . It's possible to write the cost function as a sum of three terms, one for the first leg arch, another one for the second leg, and one that allows to match the two legs.

$$\Delta V_{tot}(t_d, t_{PGA}, t_a) = \Delta V_{\oplus \rightarrow \odot}(t_d, t_{PGA}) + \Delta V_{\odot \rightarrow \star}(t_{PGA}, t_a) + \Delta V_{PGA}(t_d, t_{PGA}, t_a)$$

The first two terms are the component of  $\Delta V$  necessary to accomplish the transfer leg, calculated with the Lambert problem between the different position of the starting planet and the arrival planet

$$\Delta V_{\oplus \rightarrow \odot}(t_d, t_{PGA}) = \|\mathbf{V}_{i,leg1}(t_d, t_{PGA}) - \mathbf{V}_{\oplus}(t_d)\|$$

$$\Delta V_{\odot \rightarrow \star}(t_{PGA}, t_a) = \|\mathbf{V}_{\star}(t_a) - \mathbf{V}_{f,leg2}(t_{PGA}, t_a)\|$$

Where  $\mathbf{V}_{\star}(t_a)$  and  $\mathbf{V}_{\oplus}(t_d)$  are the velocity of Jupiter and Mercury at the corresponding instant takes from the Ephemeris data, and  $\mathbf{V}_{i,leg1}(t_d, t_{PGA}), \mathbf{V}_{f,leg2}(t_{PGA}, t_a)$  are computed through the solution of the two different Lambert problem.

In a preliminary study of the two-leg transfer, the possibility of using a multi-revolution Lambert problem has also been considered. Although no advantages have been observed in using this approach for a single transfer leg, it is possible that certain combinations of the number of revolutions before approaching the planet could lead to better optimisation of the total mission cost. However, a comprehensive study is not the focus of this design project.

The  $\Delta V_{PGA}$  component is the impulse required during the flyby in order to match the velocities at the entrance and exit of the SOI of the flyby planet:  $\mathbf{V}_{f,leg1}(t_d, t_{PGA})$  and  $\mathbf{V}_{i,leg2}(t_{PGA}, t_a)$ . In these calculations the two hyperbola inside the SOI have been made tangential; they will connect at their pericentre and it has been verified that this radius

wouldn't be minor of 100 km altitude. this manoeuvre will be called **Tangential manoeuvre**. In order to expand the considered options, if the result for a couple of Lambert arc turned out not to be valid two different flyby design have been analysed.

**Deep Space manoeuvre:** The flyby is performed with the minimum pericentre radius allowed which allows exploiting the maximum possible turning angle and the remaining rotation of the velocity comes from an impulse given at the exit of the SOI. (source: [2]).

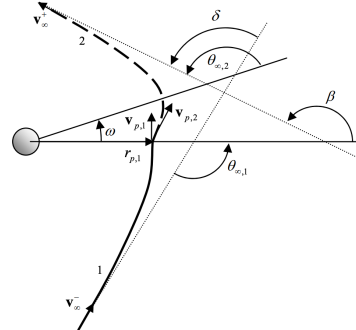
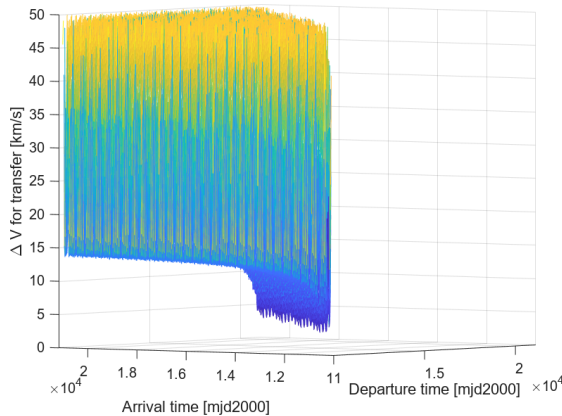


Figure 1

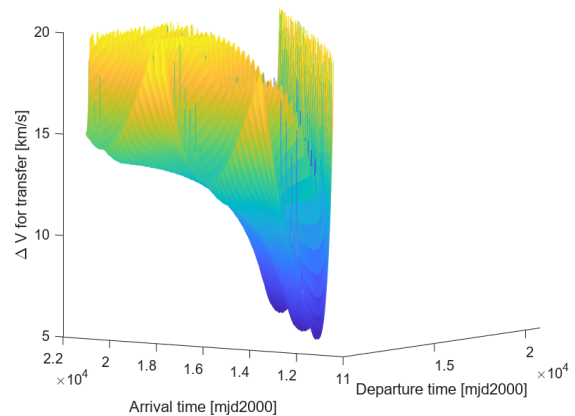
### 2.2.2 Domain

Studying the function and its domain enables the identification of patterns. It is possible to analyse not only the entire function, but also specific portions that pertain to the two transfer legs. By examining the first two terms, a pattern emerges: the cost of the manoeuvre remains consistent throughout each synodic period.

Furthermore, this data can be utilised to exclude certain portions of the domain. For instance, areas where one of the two contributions exceeds the minimum total cost of a direct transfer between Mercury and Jupiter or a specific goal parameter can be disregarded. This is a fundamental task to achieve a drastic reduction on the computational effort, but also creates a non continuous domain where a sampling strategies can perform better. This is also a strategy that can be implemented during the evaluation of the function. Instead, other strategies, like the one we are going to introduce, will not work at all. Moreover for this other method a study of the domain is very important, in order to guarantee the converge of the method in the global minimum and not in a local one. Therefore for this type of approach has been decided to express the problem through different variables  $t_d$ ,  $\text{TOF}_1$ ,  $\text{TOF}_2$ . With this change of variables it is possible to design a new domain where the interval for the second and third variables are chosen studying the two leg separately.



(a) Mesh plot for leg 1: Mercury to Earth



(b) Mesh plot for leg 2: Earth to Jupiter

Figure 2: Mesh plot for Lambert legs

It is evident from Figure 2a and Figure 2b that the cheapest combinations of departure and arrival dates for both transfer leg correspond to a restricted region of  $TOF$  values. So restricted regions have been chosen as research domain, setting a  $TOF_{min}$  and a  $TOF_{max}$  for both leg, with certain methods. Values of  $TOF$  outside of this region corresponds to costs for the single transfer leg which would unlikely lead to a minimum for the total cost of the mission. Each time this cut will be tuned with trial and error approach; approximately it falls into the range of  $0.1 \div 4$  years of  $TOF$ .

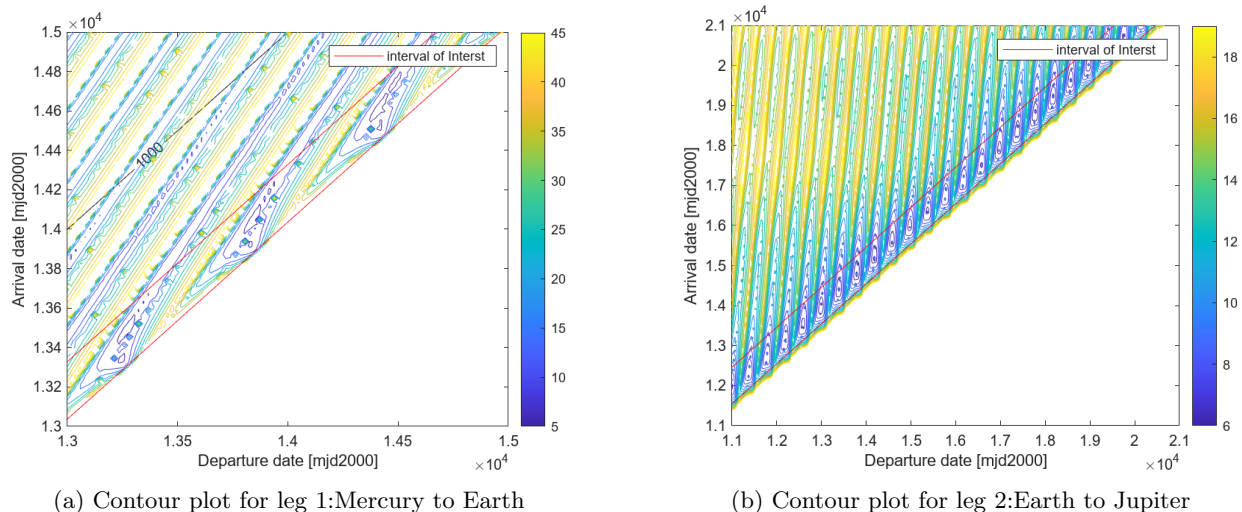


Figure 3: Example of "TOF-cut" for the two transfer legs

In Figure 3a and Figure 3b it's shown a possible cut on the domain for the two leg. In Figure 3a the two axis are limited due two graphic reason; an analogous pattern repeats itself on the full domain.

### 2.2.3 A brute force approach

To approach a problem of this type there are various methods: the simplest and most basic requires evaluating the function in many points in the reference domain and then select the point where the minimum value is found. Although this approach is easy to implement, it strongly depends on the density of the evaluation point, which depends on the number of points and of variables; in fact to reach the same density on a multidimensional domain<sup>1</sup>, it is needed a number of points that grows exponentially with the number of independent variables. The patched conics method simplifies the problem by using only three variables. However, given the search domain, a substantial number of evaluations are required to achieve a density level where the results are reliable. Consequently, this approach demands significant computational effort. Moreover, the result given by this method is typically worst than the real minimum because the sampling on the function may not be exactly in the exact point of minimum. This effect is also worst when the function has areas in the domain of interest with a pronounced gradient. This consideration has taken to implement some ideas for improving the reliability of the research and the computational effort. In order to improve the reliability, has been decided to save the best result given by the problem with a tolerance on the minimum achieved and then to use this candidates points as guess for the Matlab function `fminsearch`, when the studied problem allowed the use of this function.

`fminsearch` is a function just implemented in Matlab which allows to find the best local minimum in the guess nearby through Nelder-Mead simplex method. This has guaranteed a very high precision in the research and has led to a big improvement in the optimisation. Another strategy is a multi-grid approach in which, after the first evaluation of the function, a nearby interval of the most promising point is chosen and where the function is evaluated, unless a condition on the number of cycles or in the residual it's accomplished.

To enhance the computational efficiency of the algorithm, various strategies can be employed. One particularly effective approach involves implementing a pruning strategy during the function evaluation process, which allows to discard certain evaluation points prematurely. Specifically, if any single term within the function evaluation exceeds the current best minimum value, there is no need to compute the entire function for that particular point. Thus, a reduction in the number of function evaluations has been done. For instance, if  $\Delta V_{q \rightarrow \oplus}(t_d, t_{PGA}) > \Delta V_{min}$ , then all combinations involving this term can be pruned or discarded from further evaluation. This approach resumes the concept previously discussed regarding a cut within the search domain. In this case instead of defining a segmented search domain in advance, the cut is implemented during the function evaluation itself.

### 2.2.4 Particles Swarm optimisations

Particle Swarm Optimisation (PSO) is a population-based stochastic optimisation technique inspired by the social behaviour of birds flocking or fish schooling. In PSO, a group of potential solutions, called "particles," moves through the solution space. Each particle adjusts its position based on its own experience and the experience of neighbouring particles, aiming to converge towards the best solution in the search space. To accomplish a reliable result it has been used the PSO algorithm implemented in the Optimisation Toolbox in Matlab.

<sup>1</sup>corresponding on the same precision of results

### 2.2.5 Genetic Algorithms

In a genetic algorithm, a collection of potential solution undergoes a process of evolution aimed at improving these. Each potential solution possesses a distinct set of attributes which can undergo mutations and modifications. The evolutionary process typically commences with a set of individuals that are randomly generated. This process unfolds iteratively, with each iteration being termed as a generation. During each generation, the fitness of every individual within the population is assessed, typically based on the value of the objective function relevant to the optimisation problem. Individuals with higher fitness levels are probabilistically chosen from the existing population. Their attributes undergo modifications, involving recombination and potential random mutations, to produce a new generation of candidate solutions. This new generation then serves as the basis for the subsequent iteration of the algorithm. To accomplish a reliable result it has been used the GA algorithm implemented in the Optimisation Toolbox in Matlab.

## 2.3 Results and best option

### 2.3.1 Tangential manoeuvre

As explained in Paragraph 2.2.1 the simplest flyby manoeuvre consists in two hyperbola connected at their pericentre. A lot of these combinations will produce a not acceptable radius of pericentre which must be discarded therefore the global function to be minimised will present a lot of discontinuities. A discontinuous function can not be managed by *fminsearch* so a multi-grid brute force approach has been performed. A first execution has been performed on the whole domain. Following execution of the same brute force approach in the surrounding of the best option found led to the final solution.

GA and PSO have also been used on a restricted domain. Both algorithm didn't produce a result as good as multi-grid approach: this may be attributed to the discontinuity of the global function.

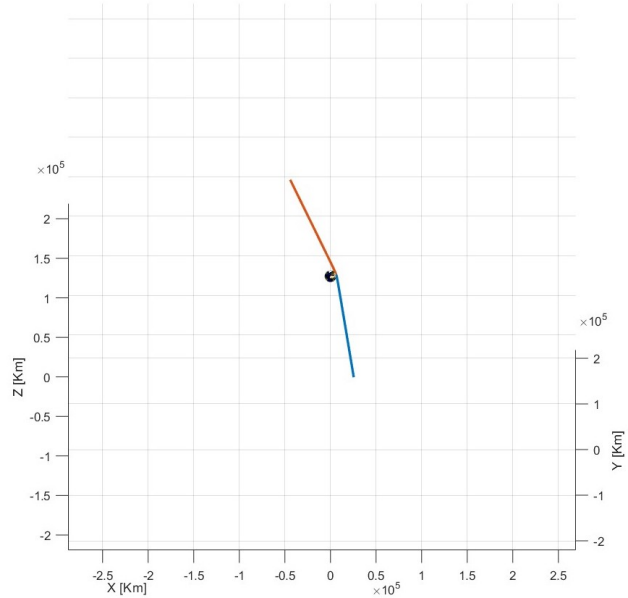
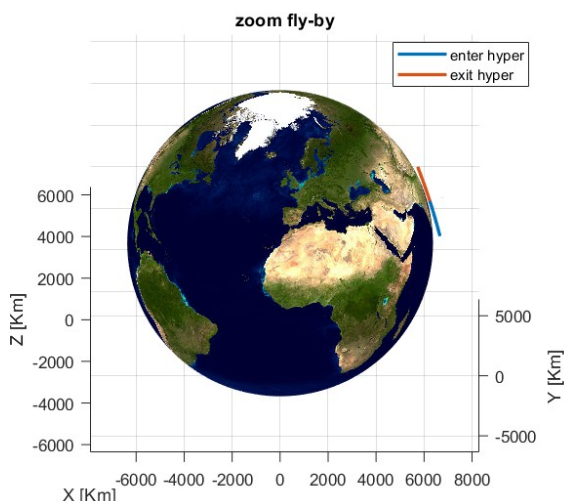
Opt. Tech.	Cost	Dep. Date	Arr. Date	GA Date
Brute	22.993695	[2036, 6, 18, 10, 25, 59]	[2041, 1, 12, 15, 52, 13]	[2038, 6, 28, 17, 33, 9]
PSO	24.207311	[2047, 7, 19, 6, 30, 22]	[2053, 6, 29, 4, 12, 18]	[2050, 7, 4, 6, 43, 17]
GA	23.487521	[2035, 12, 25, 00, 29, 40]	[2040, 12, 27, 00, 47, 46]	[2038, 6, 24, 9, 45, 55]

Table 2: Tangential manoeuvre results

The selected mission is the one obtained with brute force approach which has the following characteristics:

$$\begin{array}{lll} t_{SOI} [\text{hours}] & r_p [\text{km}] & \Delta V_{\text{powered}}/\Delta V_{GA} [-] \\ 18.851 & 6484.67 & 0.010936 \end{array}$$

Table 3: Selected flyby data



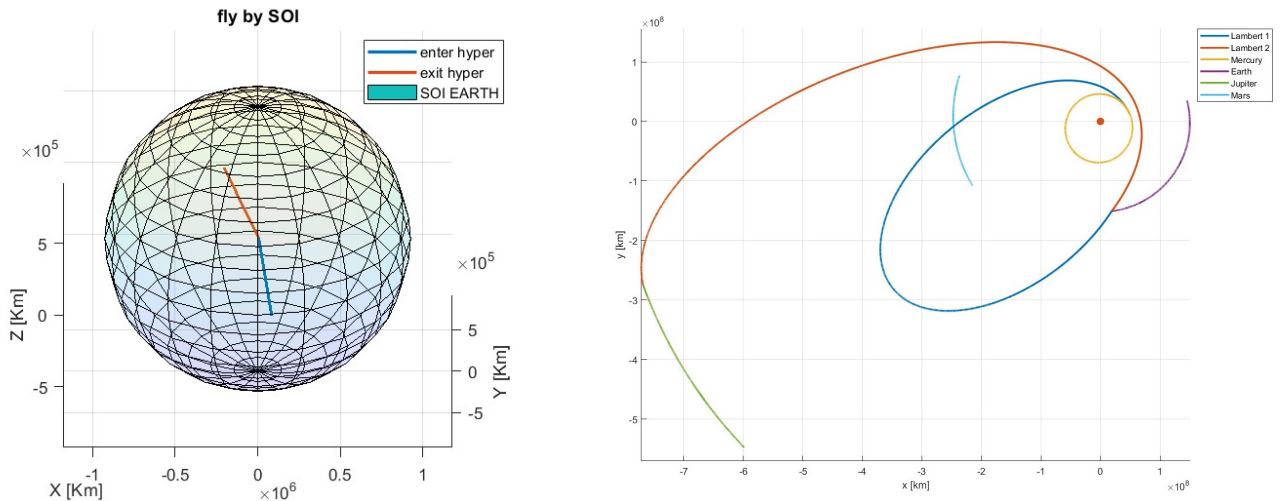


Figure 4: Selected flyby representation

### 2.3.2 Deep Space and Non Tangential manoeuvres

The Deep Space and Non Tangential flybys have been studied in order to look for alternative results. The implementation of these two flyby allowed the global function to become continuous: in this case the brute force approach has been executed only one time over the entire domain, selecting the best values. Afterwards, these values have been used as initial point for *fminsearch*, and the best of these results has been selected.

Moreover, thanks to the restored continuity of the function, PSO and GA algorithm are expected to perform better. This is the case of Non Tangent manoeuvre for which the best result has come from PSO, that gave a better result than brute force. Anyway for Deep Space manoeuvre these methods did not perform as good as the brute force approach.

Opt. Tech.	Cost	Dep. Date	Arr. Date	GA Date
Brute	22.835042	[2036, 6, 19, 14, 11, 25]	[2041, 2, 3, 3, 12, 60]	[2038, 6, 29, 20, 26, 18]
PSO	24.062851	[2036, 9, 16, 6, 8, 23]	[2040, 2, 3, 15, 34, 8]	[2037, 6, 20, 16, 1, 19]
GA	23.168167	[2048, 1, 7, 18, 59, 22]	[2052, 2, 27, 1, 8, 46]	[2049, 6, 12, 23, 26, 4]

Table 4: Deep Space manoeuvre results

Opt. Tech.	Cost	Dep. Date	Arr. Date	GA Date
Brute	15.076080	[2034, 1, 22, 23, 50, 6]	[2037, 2, 24, 0, 21, 42]	[2034, 5, 23, 23, 40, 21]
PSO	14.780125	[2045, 2, 28, 0, 44, 8]	[2047, 10, 20, 18, 43, 3]	[2045, 5, 12, 23, 47, 54]
GA	15.135276	[2033, 2, 7, 7, 30, 51]	[2035, 9, 28, 19, 29, 1]	[2033, 5, 7, 18, 2, 55]

Table 5: Non Tangential manoeuvre results

It's truly impressive the total cost obtained with the Non Tangential flyby manoeuvre. Anyway it has not been selected because of the assignment requests.

### 3 Planetary observation mission

"The PoliMi Space Agency wants to launch a Planetary Explorer Mission, to perform Earth observation. As part of the mission analysis team, you are requested to carry out the orbit analysis and ground track estimation. You have to study the effects of orbit perturbations, and compare different propagation methods. Also, you have to characterise the ground track, and propose an orbit modification to reach a repeating ground track (for better communications with our network of ground stations)."

#### 3.1 Requirements

The planet observed by this mission is the Earth and the orbit is assigned through the values of semi-major axis  $a = 26557$  km, eccentricity  $e = 0.7020$  and inclination  $i = 61.9721$  deg; while the values of RAAN  $\Omega$ , anomaly of the pericentre  $\omega$  and initial true anomaly  $\theta$  are not constrained.

The perturbations to be accounted are the  $J_2$  effect, i.e. the second zonal harmonic due to Earth oblateness, and the Solar Radiation Pressure (SRP) given the following s/c parameters: surface over mass  $A/m = 5.0000m^2/kg$  and reflectivity coefficient  $C_r = 1.0$ .

The desired Repeating Ground Track has a  $k : m$  ration of 2 : 1; where k and m are respectively the number of revolution after which the ground-track repeat and the number of day or frequency after which this occurs.

#### 3.2 Initial orbit characterisation

The initial orbit has been propagated setting the following orbital elements at epoch 2028/01/01.

$a$ [km]	$e$ [-]	$i$ [deg]	$\Omega$ [deg]	$\omega$ [deg]	$\theta$ [deg]
26557	0.7020	61.9721	25	8	0

Table 6: Orbital elements of initial orbit.

This orbit of the s/c around the Earth - which is propagated as an unperturbed two-body problem - produces the following ground track:

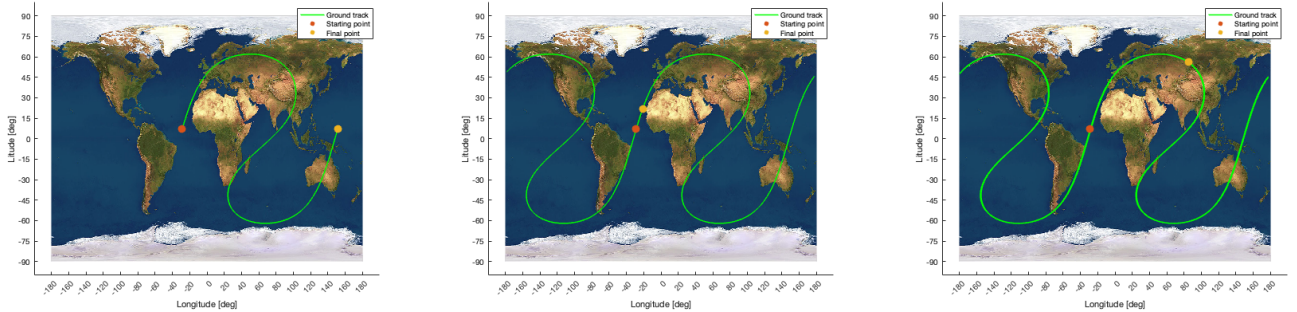


Figure 5: Unperturbed initial orbit ground track over 1 period, 1 day and 10 days

The perturbations affect the orbit through the following perturbing accelerations:

- $J_2$  effect:

$$\mathbf{a}_{J_2} = \frac{3}{2} \frac{J_2 \mu R_e^2}{r^4} \left[ \frac{x}{r} \left( 5 \frac{z^2}{r^2} - 1 \right) \hat{\mathbf{i}} + \frac{y}{r} \left( 5 \frac{z^2}{r^2} - 1 \right) \hat{\mathbf{j}} + \frac{z}{r} \left( 5 \frac{z^2}{r^2} - 3 \right) \hat{\mathbf{k}} \right] \quad (1)$$

- SRP effect:

$$\mathbf{a}_{SRP} = -eclipse \cdot p_{sr@1AU} \frac{AU^2}{||\mathbf{r}_{sc \rightarrow O}||^3} \mathbf{r}_{sc \rightarrow O} \cdot c_R \frac{A_O}{m} \quad (2)$$

It can be noticed that the equation takes into account whether the s/c is in eclipse or not through the *eclipse* parameter. The conditions for the eclipse follows the model proposed by Wertz in [6], which also provides the formulas to compute the fraction of solar radiation reaching the s/c in case of partial and annular eclipse.

The orbit propagated with perturbations produces the following ground tracks:

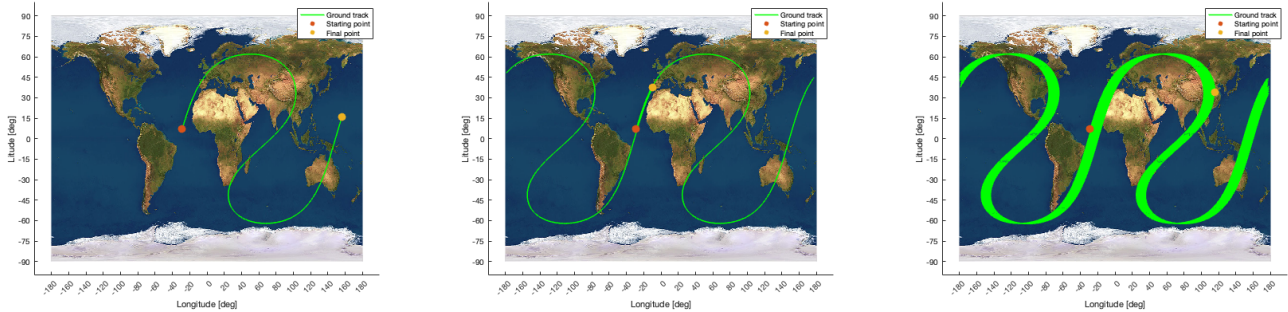


Figure 6: Perturbed initial orbit ground track over 1 period, 1 day and 10 days

### 3.3 Ground track repeating orbit characterisation

In order to have a ground track that will repeat itself after a certain number of rotations, it is possible to modify the semi-major axis of the orbit (i.e. its period) making the total ground track drifting during  $k$  revolutions equal to the corresponding planet rotations during  $m$  days. With  $\Delta\lambda$  being the ground track shift per period, the condition to be respected is

$$k\Delta\lambda = m2\pi \quad \Rightarrow \quad \frac{\Delta\lambda}{2\pi} = \frac{m}{k} \quad \text{with } k, m \in \mathbb{N} \quad (3)$$

In the case of unperturbed two-body problem, during one orbital period  $T$  the ground track advances westward by an angle  $\Delta\lambda$  equal to the Earth angular rotation  $\omega_{\oplus}$  during that time, so:  $\Delta\lambda = T\omega_{\oplus}$ . It is also known that Earth's rotational period is  $T_{\oplus} = 2\pi/\omega_{\oplus}$ . Substituting these expressions in (3):

$$\frac{T}{T_{\oplus}} = \frac{m}{k} \quad \text{with } k, m \in \mathbb{N} \quad (4)$$

The value of semi-major axis coming from this condition is  $a_{rep,unpert} = 26561.76$  km, which produces a perfect repeating ground track when propagated unperturbed. When introducing perturbations, the angular precession of the orbit due to J2 effect creates another component of drift in the ground track: the ground track will no longer perfectly repeat itself.

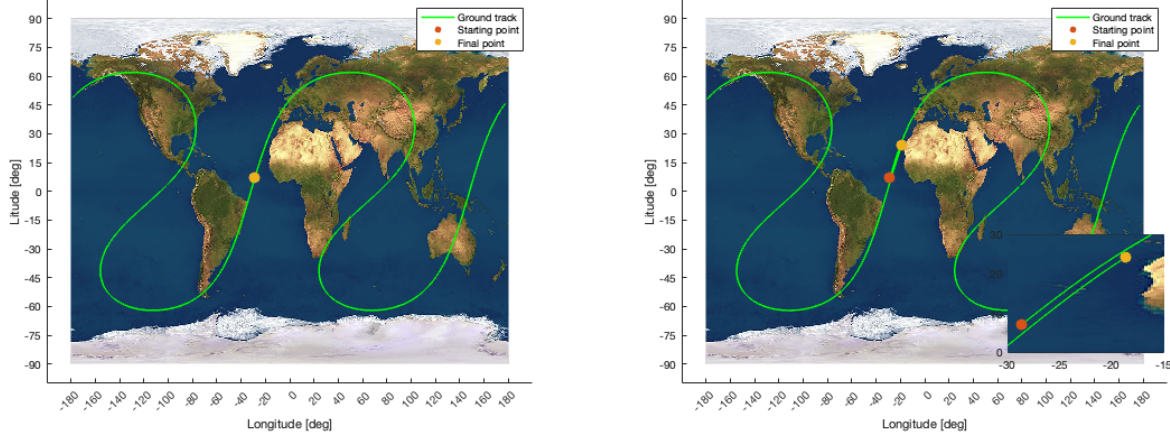


Figure 7: Ground track for  $a_{rep,unpert}$  semi-major axis over 2 period. Propagated unperturbed (left) and perturbed (right)

It is possible to include in the shift correction also the component due to gravity field perturbation. The ground track shift  $\Delta\lambda$  is now considered between two consecutive equator crossing points, which will occur after one *nodal period*  $P_{\Omega}$ , and it is given by the sum of the effect of Earth angular rotation  $\omega_{\oplus}$  and the nodal shift  $\dot{\Omega}$  due to J2 effect (source: [5]).

$$\Delta\lambda = (\omega_{\oplus} + \dot{\Omega})P_{\Omega} \quad (5)$$

By substituting this expression in Eq. (3) with the nodal period defined as  $P_\Omega = \frac{2\pi}{n + \dot{M}_0 + \dot{\omega}}$  it is obtained the new condition for repeating ground track:

$$\frac{\omega_\oplus + \dot{\Omega}}{n + \dot{M}_0 + \dot{\omega}} = \frac{m}{k} \quad (6)$$

The following definitions for the secular perturbations of the RAAN, the anomaly of perigee and the mean anomaly have been used (source: [5]):

$$\dot{\Omega} = -\frac{3nR_\oplus^2 J_2}{2a^2(1-e^2)^2} \cos i \quad (7)$$

$$\dot{M}_0 = \frac{3nR_\oplus^2 J_2 \sqrt{1-e^2}}{4a^2(1-e^2)^2} \left( 3\sin^2 i - 2 \right) \quad (8)$$

$$\dot{\omega} = \frac{3nR_\oplus^2 J_2}{4a^2(1-e^2)^2} \left( 4 - 5\sin^2 i \right) \quad (9)$$

By solving equation 6 for the semi-major axis, it is obtained a value of  $a_{rep,pert} = 26568.91$  km, which produces the ground track shown in Figure 8 when propagated in the perturbed two-body problem.

It is noticeable from the zoom that the ground track is still not perfectly repeating itself.

This behaviour is due not only to the disturbance of SRP but to the fact that equation 6 is working only with the secular effect of the gravity field perturbation, without considering the long-period oscillation.

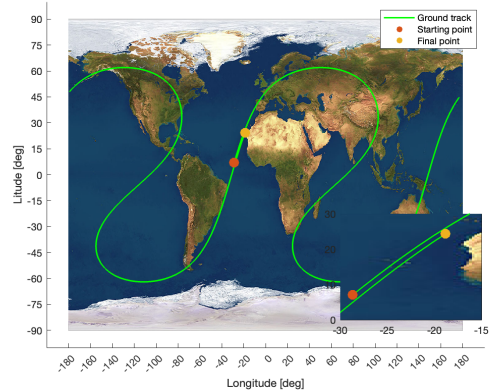


Figure 8

### 3.4 Orbital elements propagation and filtering

The orbit has been propagated along 1 year with starting epoch set at 01/01/2028 in order to see its evolution due to the effect of perturbations. Two different methods can be used

**Cartesian coordinates:** Integration of the equation of motion in Cartesian coordinates expressed in the form:

$$\frac{d^2\mathbf{r}}{dt^2} = -\frac{\mu}{r^3}\mathbf{r} + \sum \mathbf{a}_{pert} \quad (10)$$

The result of this integration is the evolution of position and velocity vectors. So it is possible to plot the 3D representation of the orbit evolution. Figure 9 shows the evolution of the orbit during 1 year.

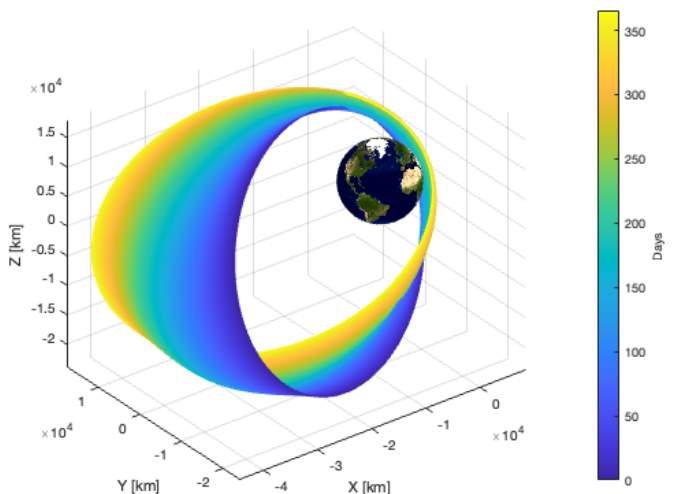


Figure 9

**Gauss planetary equations:** Integration of the equations of motion of singular orbital elements ( $a, e, i, \Omega, \omega, \theta$ ). Their expression in TNH (tangential – normal – out-of-plane) reference frame has been used (source: [4]). The output of this integration is the evolution of the Keplerian elements so it is possible to plot it. (The evolution of the orbital elements can be seen in the Figure 11)

### 3.4.1 Cartesian coordinates VS Gauss planetary equations

Since the evolution of the orbital elements can be recovered also from the Cartesian coordinates through the *car2kep* function, a comparison between the two methods will be held. The comparison has been done for both *ode113* and *ode45* Matlab integrator, since its choice hugely affects the results.

The discrepancy between the two method can be evaluated as the infinity norm of the difference between the values coming from the two methods.

	$a$ [km]	$e$ [-]	$i$ [deg]	$\Omega$ [deg]	$\omega$ [deg]	$\theta$ [deg]
$ \text{diff} _\infty$	4.34e-04	4.82e-09	4.30e-08	6.04e-08	2.94e-07	1.93e-04

Table 7: Infinity norm of the difference over 1 year with *ode113*

	$a$ [km]	$e$ [-]	$i$ [deg]	$\Omega$ [deg]	$\omega$ [deg]	$\theta$ [deg]
$ \text{diff} _\infty$	1.30e-03	1.43e-08	1.22e-07	1.52e-07	8.52e-07	5.41e-04

Table 8: Infinity norm of the difference over 1 year orbit with *ode45*

It is also possible to compare the computational efficiency in terms of time of execution as function of number of orbits integrated.

Figure 10 shows the execution time for Gauss and Cartesian methods as function of number of days integrated; both for *ode113* and *ode45*. From the plot it's clear that *ode113* performs definitely better when compared to *ode45*. It can be also observed that Cartesian and Gauss methods take the same time when using *ode113* while the required time by *ode45* with Cartesian method increases faster than with Gauss.

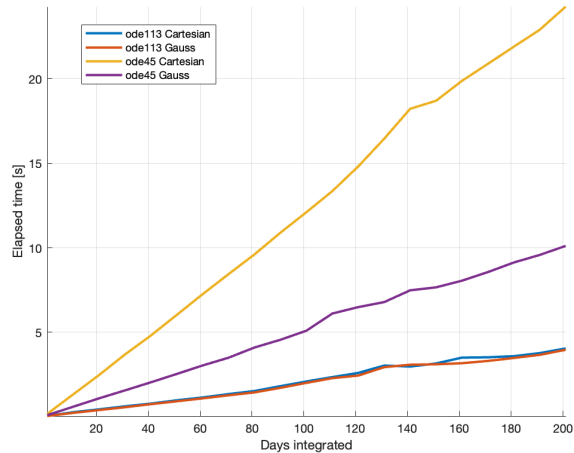


Figure 10

### 3.4.2 Filtering

Each perturbation can have several characteristic periods which will affect the orbital elements in different timescales. The global evolution of each orbital element will be the composed of the summation of all of the frequencies. It is possible to filter the results of the numerical propagation in order to visualise only their relevant frequencies.

Two different filtering methods have been used: the **Fast Fourier Transform (FFT)** and the **Moving Average (movmean)**.

**Moving Average:** This method, performed with Matlab function *movmean*, computes the local mean in a moving fixed size window of points. Changing the size of the window it is possible to decide how much to attenuate the oscillation.

**Fast Fourier Transform** Using this method it is possible to operate as a proper low-pass filter on the signal, deleting all the frequency components over a certain value. That has been done with Matlab function *FFT* and *IFFT*, in order to convert the signal from the time-domain representation to its frequency-domain representation and vice versa.

The following results have been obtained tuning the two methods with a trial and error approach.

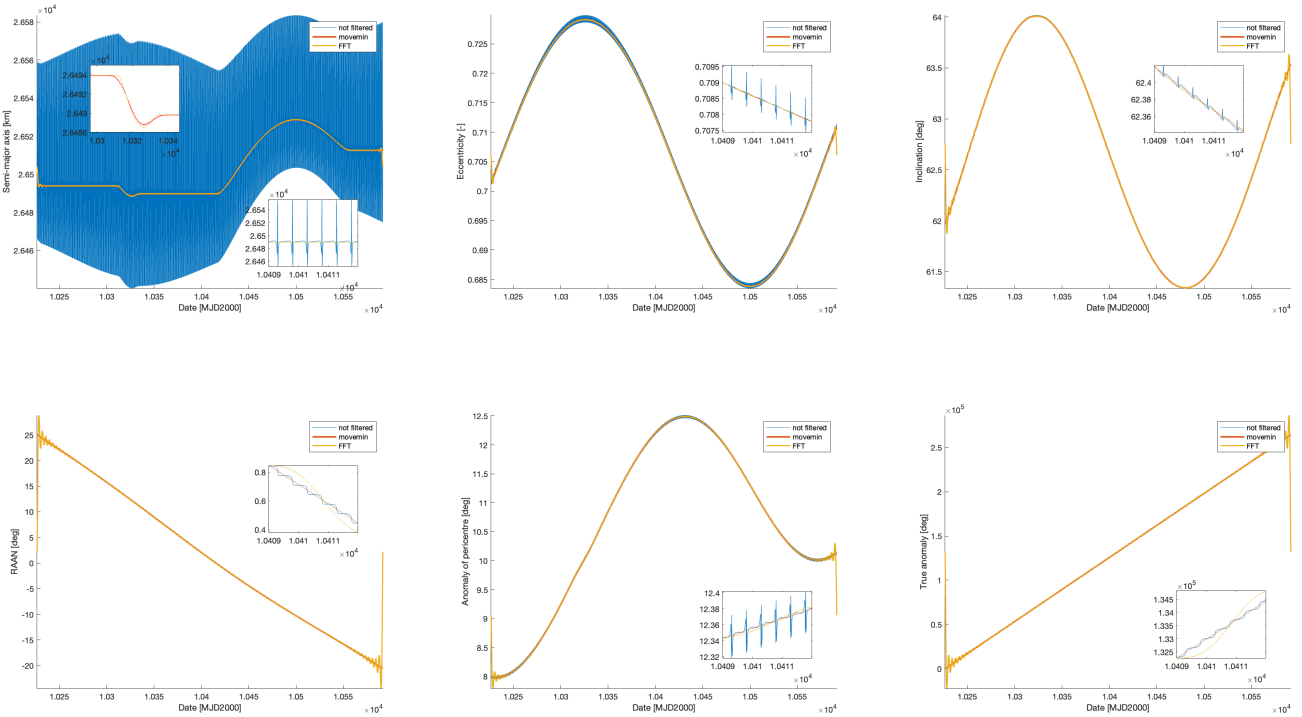


Figure 11: Evolution of the orbital elements during 1 year

It can be seen that *FFT* filtering presents some criticism. First of all at the border of the domain the filtered signal oscillates a lot due to the Gibbs phenomenon. Moreover, the more low frequencies are filtered out, the more oscillations grow in amplitude. Instead, the more high frequencies are kept, the more the new signal overlaps the initial one. Those cases do not provide good filtered data. Instead, *movemin* provides a much smoother signal.

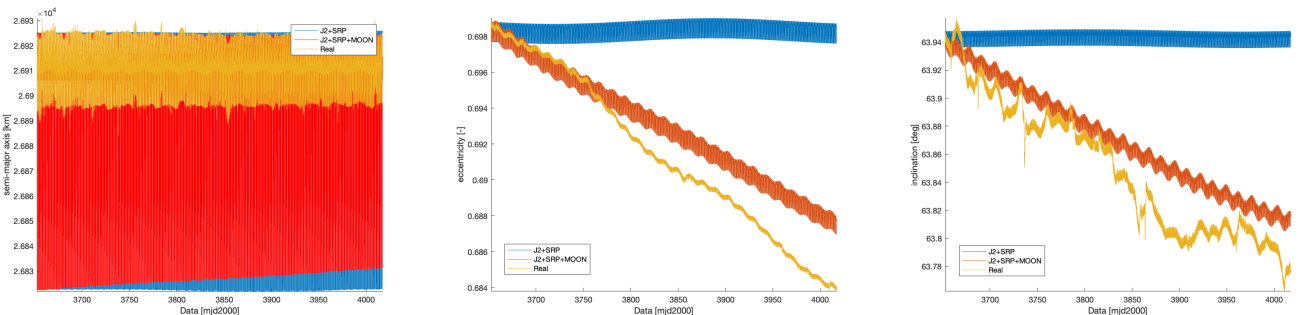
### 3.5 Comparison with real data

In order to validate the model used for orbit propagation, a comparison with real data download from NASA Horizon database has been performed.

The object selected is the rocket body debris NORAD: 25850 (coming from the mission Molniya-3 63L launched on 1999-07-08). This choice is based on the fact that its orbit is very similar to our mission's one. The parameters for the SRP have been assumed as  $A/m = 0.030m^2/kg$  and the reflectivity coefficient  $C_r = 1.0$ . The  $A/m$  coefficient has been computed using general data from the launcher vehicle Molniya-M (Blok-ML) (8K78M) (source: [1]).

The orbit evolution has been downloaded from the online database in terms of position and velocity. Through *car2kep* the evolution of Keplerian elements has been recovered and compared to the data obtained from the model. As shown in Figure 12, the real eccentricity and inclination present a drift that, instead, the model with J2 and SRP disturbances is not capable of computing. This could be attributed to the absence of the third-body perturbation due to the Moon. In order to verify this hypothesis, the effect of the gravitational attraction of the Moon has been included (see equation 11). After introducing this effect, the data coming from the model displays the same trend as the real ones.

$$\mathbf{a}_\mathbb{D} = \mu_\mathbb{D} \left( \frac{\mathbf{r}_{s/c \rightarrow \mathbb{D}}}{r_{s/c \rightarrow \mathbb{D}}^3} - \frac{\mathbf{r}_{\oplus \rightarrow \mathbb{D}}}{r_{\oplus \rightarrow \mathbb{D}}^3} \right) \quad (11)$$



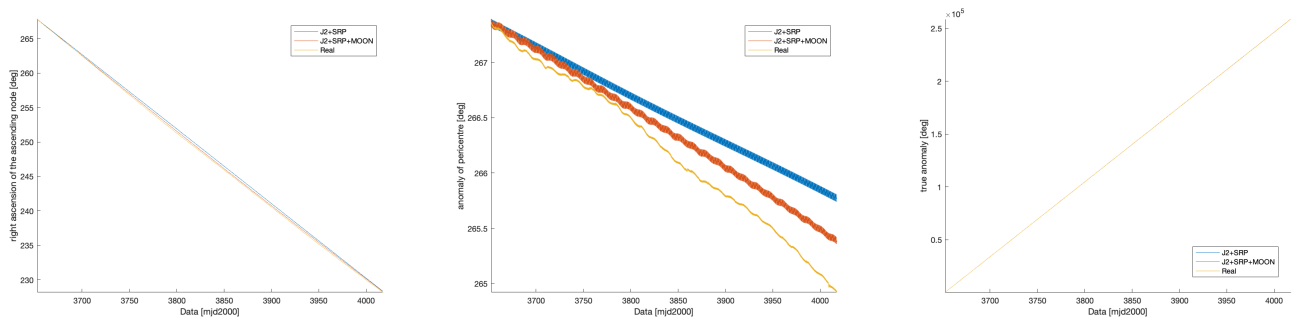


Figure 12: Keplerian elements evolution: real vs J2+SRP perturbed vs J2+SRP+MOON perturbed

## References

- [1] *Astronautix.com*. URL: <http://www.astronautix.com/m/molniya8k78m.html>.
- [2] Andrea Caruso. *Ottimizzazione di Traiettorie Interplanetarie con Manovre Impulsive. Tesi Magistrale*. <https://etd.adm.unipi.it/theses/available/etd-05202016-105223/unrestricted/Tesi.pdf>. 2016.
- [3] Matteo Ceriotti. *Global optimisation of multiple gravity assist trajectories*. PhD thesis. [https://strathprints.strath.ac.uk/26349/1/Ceriotti\\_M\\_strathprints\\_Global\\_optimisation\\_of\\_multiple\\_gravity\\_assist\\_trajectories\\_PhD\\_Thesis\\_2010.pdf](https://strathprints.strath.ac.uk/26349/1/Ceriotti_M_strathprints_Global_optimisation_of_multiple_gravity_assist_trajectories_PhD_Thesis_2010.pdf). 2010.
- [4] Giacomo Borelli Lorenzo Giudici Mathilda Bolis Juan Luis Gonzalo Gomez Camilla Colombo. *Lab Chapter 5: Orbit perturbations*. 2023/2024.
- [5] David A. Vallado. *Fundamental of Astrodynamics and Application*. Space Technology Series, 2013.
- [6] James R. Wertz. *Spacecraft Attitude Determination and Control Volume 73 of Astrophysics and Space Science Library*. Springer Science Business Media, 1978.